



ACDIV-2018-02

January 2018

Latest developments at the ALBA magnetic measurements laboratory

J. Marcos, V. Massana, L. García and J. Campmany

Abstract

ALBA is a third-generation synchrotron light source that has been in operation since 2012 near Barcelona. A magnetic measurements laboratory has been associated with the facility since its very early stages and has been active for the last 20 years. In the first part of this work, the different instruments available at the laboratory are described, and a brief overview of the measurement campaigns carried out during its 20 years of history is presented. In the second part, a more detailed description of the approach to Hall probe measurements adopted at ALBA is offered, with an explanation of the methods and ancillary equipment that have been developed along the years in order to improve the accuracy of the system. In the third part, a new concept of Hall probe bench devoted to the measurement of closed structures is presented. The in-house design and building of a prototype for such a bench is described, together with its mechanical and magnetic characterization. As a conclusion, the first results obtained with this bench are discussed.

Accelerator Division
Alba Synchrotron Light Source
c/ de la Llum, 2-26
08290 Cerdanyola del Valles, Spain

Latest developments at the ALBA magnetic measurements laboratory

J Marcos¹, V Massana, L García and J Campmany

CELLS, ALBA Synchrotron, Carrer de la Llum 2-26, E08290, Cerdanyola del Vallès, Barcelona, Spain

E-mail: jmarcos@cells.es

Received 12 July 2017, revised 25 August 2017

Accepted for publication 11 September 2017

Published 17 January 2018



CrossMark

Abstract

ALBA is a third-generation synchrotron light source that has been in operation since 2012 near Barcelona. A magnetic measurements laboratory has been associated with the facility since its very early stages and has been active for the last 20 years. In the first part of this work, the different instruments available at the laboratory are described, and a brief overview of the measurement campaigns carried out during its 20 years of history is presented. In the second part, a more detailed description of the approach to Hall probe measurements adopted at ALBA is offered, with an explanation of the methods and ancillary equipment that have been developed along the years in order to improve the accuracy of the system. In the third part, a new concept of Hall probe bench devoted to the measurement of closed structures is presented. The in-house design and building of a prototype for such a bench is described, together with its mechanical and magnetic characterization. As a conclusion, the first results obtained with this bench are discussed.

Keywords: synchrotron light sources, magnetic measurements, Hall probes, accelerator magnets

(Some figures may appear in colour only in the online journal)

1. Introduction

ALBA is a third-generation synchrotron light source that has been open to users since 2012 in Cerdanyola del Vallès, close to Barcelona [1]. It operates at an electron beam energy of 3 GeV, and it is currently running eight beamlines, with an additional one under construction and two more with their budget approved and in design phase.

A laboratory for the testing and development of magnetic structures has existed since 1996 and was associated with the project to build a synchrotron light source in the Barcelona area, first located at the premises of Universitat Autònoma de Barcelona (UAB) and afterwards moving to the ALBA site in 2009. At its present location, the laboratory occupies an enclosed space with an area of 150 m² and it is equipped with an independent air conditioning system, which provides a temperature stability of ± 0.1 °C.

The laboratory has different available systems for the characterization of magnetic structures:

- A Hall probe bench produced by Ramem on 1997, providing 3D magnetic field-mapping capabilities along a longitudinal range of 3 m. It is used as a general-purpose bench for determining the local value of the magnetic field.
- A rotating coil bench purchased from CERN in 2008, which allows determining the integrated field and its harmonics on magnets with lengths of up to 0.5 m.
- A flipping coil bench produced by ESRF in 2006, which is used to determine low-value field integrals from small gap devices. This is a bench oriented to the characterization of insertion devices.
- A set of Helmholtz coils produced by Elettra in 2006 and a fixed stretched wire developed in-house in 2007, used to characterize permanent magnet blocks prior to their assembly into insertion devices.

During its 20 years of activity, the laboratory has been involved in many measurement campaigns aimed at the characterization of magnets both for the ALBA project and for other projects and institutions. Among the most relevant

¹ Author to whom any correspondence should be addressed.

campaigns are the measurement of: (i) the bending magnets ($\times 16$) of the ANKA storage ring (1998–1999) [2]; (ii) the bending magnets ($\times 24$) of the Canadian Light Source (CLS) storage ring (2001–2002) [3]; (iii) the bending magnets ($\times 32$) of the ALBA storage ring (2007–2008); (iv) the insertion devices for the phase-I beamlines at ALBA (2009–2010); (v) the bending magnets ($\times 16$) of the SESAME storage ring (2014–2015) [4]; (vi) the quadrupoles ($\times 5$) for the medium energy beam transfer of LIPAc accelerator [5]; and (vii) the dipoles ($\times 15$) and quadrupoles ($\times 34$) of the accelerators for the ThomX facility (2016). In most cases the main instrument used for the characterization of magnets was the Hall probe bench, typically through detailed mapping of the field within the midplane of the magnet. For this reason, in this paper we will focus on the approach used at ALBA for measurements with Hall probes.

2. Hall probe measurements at ALBA

2.1. Magnetic field measurement with Hall sensors

In a Hall-effect sensor, a voltage difference is created across an electrical conductor transverse to the electric current flowing through it and to the magnetic field in the direction perpendicular to the current [6]. The situation is illustrated in figure 1. Ideally, the generated Hall voltage V_H is proportional to the magnetic field component perpendicular to the surface of the sensor, i.e.

$$V_H(B_z) = I_c \frac{R_H}{t} B_z = S B_z, \quad (1)$$

where I_c is the control current flowing through the sensor, t is the sensor thickness, R_H is the Hall coefficient depending on intrinsic parameters of the sensor's material, B_z is the magnetic field component perpendicular to the sensor, and S is the resulting magnetic sensitivity providing the proportionality factor between the field to be measured and the generated voltage. For an n-type semiconductor, the Hall coefficient is given by $R_H = -1/(qn) = -\mu_n/\sigma$, where n is the density of charge carriers (electrons), μ_n is their electrical mobility, and σ is the electrical conductivity of the material. In order to have a high value of R_H , materials with high mobility and low conductivity such a silicon or gallium arsenide are customarily chosen.

In a real situation, however, there are several deviations from the ideal linear behaviour:

- In the absence of a magnetic field, the measured voltage is different from zero. This so-called offset voltage is associated with structural asymmetries of the active part of the Hall sensor (either errors in the geometry or in the doping homogeneity) and it is also influenced by temperature gradients, mechanical stresses and ageing effects. As a result of this combination of factors, the offset voltage displays a drift along time.
- The Hall coefficient of the sensor's material depends on temperature, leading to a thermal dependence of the sensitivity of the sensor.

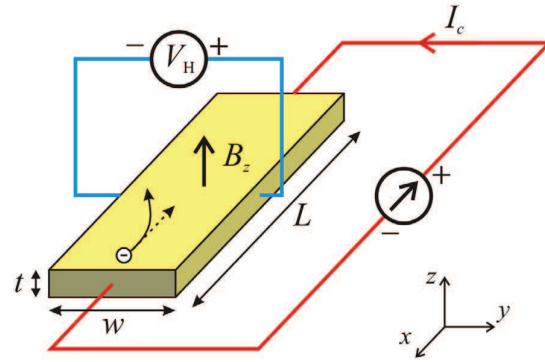


Figure 1. Diagram illustrating the Hall effect and governing parameters.

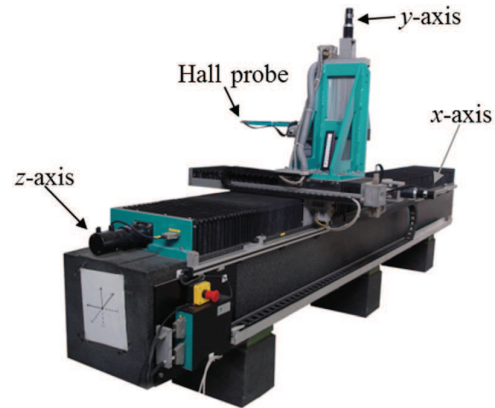


Figure 2. View of the conventional Hall probe bench at the ALBA magnetic measurements laboratory.

- The Hall voltage has an additional contribution from the magnetic field component within the plane of the sensor, known as the planar Hall effect. Taking the axes configuration shown in figure 1, the planar Hall effect is proportional to the product of the two in-plane field components, $B_x B_y$, with a proportionality constant usually referred to as the planar Hall coefficient c_p .

On top of these effects, there are nonlinearities and higher-order cross-terms. Therefore, in general, the Hall voltage in a real situation can be expressed as

$$V_H(B_x, B_y, B_z) = V_{\text{offset}} + S(T)B_z + c_p B_x B_y + o(B^2), \quad (2)$$

where the term $o(B^2)$ stands for the contribution of the nonlinear terms excluding the planar Hall effect. These deviations from ideal behaviour have to be properly taken into account in order to reach relative accuracy in the determination of the magnetic field in the range of 10^{-4} .

2.2. Hall probe bench at ALBA

The Hall probe bench at ALBA, shown in figure 2, consists of three orthogonal linear stages mounted one on top of each other covering a scanning volume of $\Delta x \times \Delta y \times \Delta z = (500 \times 250 \times 3000) \text{ mm}^3$. The three axes are driven by DC motors, and the motion system is controlled by a PMAC unit. Attached

to the third linear stage is an aluminum profile arm on top of which different Hall probes can be mounted, depending on the geometry of the magnet to be measured. The bench was originally built in 1997 [7] and over the years it has undergone several hardware and software upgrades in order to improve its performance.

In all cases, the Hall probes at ALBA consist of an in-house PCB board with three orthogonally mounted uniaxial commercial Hall sensors. Gallium arsenide planar sensors of GH-series (GH-700 and GH-701 models) from FW Bell are typically used, with a magnetic sensitivity of $S \sim 1 \text{ V T}^{-1}$ for a control current of 5 mA, and a sensitive area with a diameter of 0.3 mm. The three sensors are powered in series using a high stability current supply, and the generated Hall voltages are recorded using Keithley 2001 voltmeters, with a resolution of $7\frac{1}{2}$ digits. The overall thickness of the probes is typically kept below 4 mm in order to allow the measurement of small gap devices such as in-vacuum undulators.

From a software point of view, the control system has been implemented using TANGO, and it allows measuring both statically and dynamically whilst the longitudinal axis is moving (on-the-fly measurement mode) for velocities up to 16 mm s^{-1} .

2.3. Approach to Hall probe measurements at ALBA

In order to be able to map a 3D magnetic field with good precision using the Hall probe, with a high accuracy both in the positioning of the probe and in the determined field values, there are several difficulties that must be addressed:

1. Thermal dependence of the Hall coefficient.
2. Nonlinearities and cross-terms between magnetic field components.
3. Non-zero offset voltage drifting with time.
4. Relative positioning of Hall sensors in the case of using several uniaxial sensors.
5. Absolute position of the Hall probe with respect to the laboratory system of reference.
6. Orientation of the Hall probe with respect to the laboratory system of reference.

In this section we will describe the solutions implemented at ALBA to solve or mitigate all these issues.

2.3.1. Thermal dependence. The gallium arsenide Hall sensors used at ALBA have a temperature coefficient for their magnetic sensitivity of $\alpha_T = -(1/S)(dS/dT) \sim 0.07\%/^\circ\text{C}$. In order to get rid of this thermal dependence, a Pt-100 temperature sensor and a heater are also mounted on the circuit board of the Hall probes, as shown in figure 3. These elements, in combination with a PID controller (Eurotherm 3508), allow one to keep the temperature of the probe within $\pm 0.05 \text{ }^\circ\text{C}$. In addition, during the calibration process of the Hall probe, the temperature coefficient of the sensitivity is determined for each sensor assuming a linear dependence, i.e. $S(T) = S(T_0) [1 - \alpha_T (T - T_0)]$, where T_0 is the reference temperature of the probe. In this way any residual temperature deviation during a measurement can be adequately taken into account.

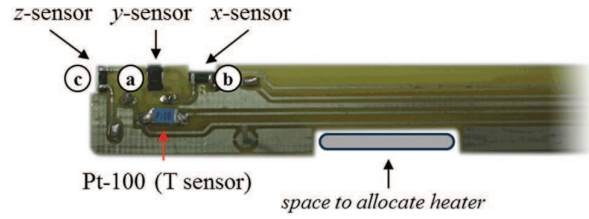


Figure 3. Diagram of a typical Hall probe used at ALBA.

2.3.2. Hall probe calibration. In order to reproduce the response of the Hall probe to an arbitrary field, a parametric model based on equation (2) is used that takes into account nonlinearities, cross-terms between magnetic field components (planar Hall effect and higher-order terms), and the non-orthogonality between the three Hall sensors mounted on the circuit board. The Hall voltage generated on each sensor of the probe is thus expressed in terms of the three components of the external magnetic field:

$$\begin{cases} V_a = V_a(B_x, B_y, B_z, T) \\ V_b = V_b(B_x, B_y, B_z, T) \\ V_c = V_c(B_x, B_y, B_z, T) \end{cases}, \quad (3)$$

where the sensor labelling shown in figure 3 has been used. By applying magnetic fields of known intensity inside a calibration magnet for different orientations of the Hall probe, it is possible to determine all the parameters characterizing the response of each sensor. Afterwards, an arbitrary magnetic field can be reconstructed from the voltages measured on the three sensors by solving the nonlinear system of equations in equation (3).

In order to perform the calibration, we use a dipole magnet GMW 3473-50 150 mm providing magnetic fields up to 1.7 T, and as a standard for the determination of the magnetic field level we use NMR probes and a PT2025 magnetometer from Metrolab, which is specified to determine magnetic field with an accuracy within 5×10^{-6} .

Typical residual errors between the calibration data and the adjusted parametric model are of the order of $20 \mu\text{T}$ rms. As a result, the overall accuracy level of our Hall probes in the calibrated range is within 1×10^{-4} .

2.3.3. Offset voltage. It has been determined that the offset of the Hall sensors used at ALBA drifts up to $10 \mu\text{T}$ within a working day, and up to $50 \mu\text{T}$ from one day to the next, making it advisable to measure the probe offset before and after any long measurement. In order to perform this offset determination, a double-layered μ -metal chamber defining a zero magnetic field region inside it was designed and constructed in-house. When the probe is introduced inside the chamber, the voltage readings of the three Hall sensors provide a direct measurement of their offsets. The chamber and the offset-determination procedure are shown in figure 4. The selected material for the walls of the chamber was 80%Ni-Fe μ -metal with a thickness of 1.575 mm. The chamber provides a shielding factor of the external field of ~ 1500 along its radial direction and ~ 700 along its axial direction.

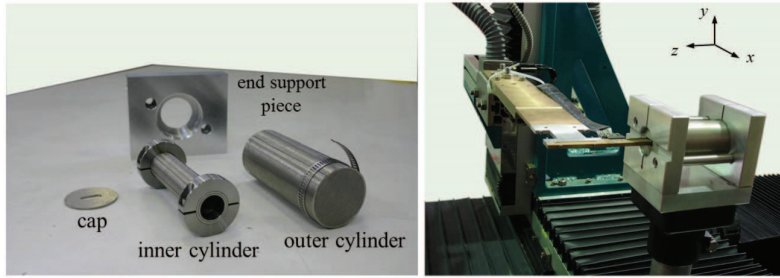


Figure 4. Left: Piece breakdown of the zero-field magnetic chamber for offset determination. Right: Illustration of offset measurement procedure.

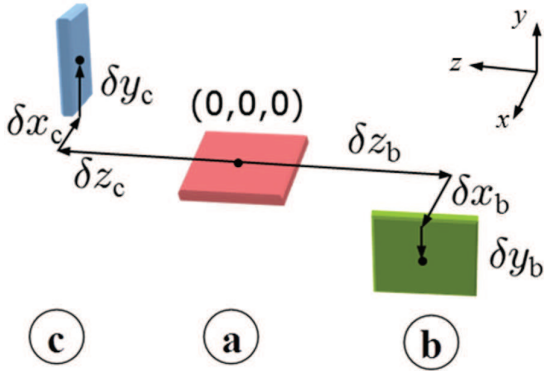


Figure 5. Relative positions of the three sensors mounted on a Hall probe, taking the vertical sensor measuring B_y as a reference.

2.3.4. Relative distances between Hall sensors. In order to measure the three components of the magnetic field at a given point, it is necessary to know the relative distances between the sensitive areas of the three Hall sensors mounted on the circuit board of the probe, as illustrated in figure 5. A self-consistent method based on the fulfilment of Maxwell equations has been developed which allows determining those distances.

In effect, any magnetic field in a region free of sources must fulfil the corresponding Maxwell equations:

$$\begin{cases} \vec{\nabla} \cdot \vec{B} = 0 \\ \vec{\nabla} \times \vec{B} = 0 \end{cases} \quad (4)$$

Therefore, the following combinations of field-derivatives must be identically zero:

$$\begin{cases} f_1(\vec{r}) = \partial_x B_x(\vec{r}) + \partial_y B_y(\vec{r}) + \partial_z B_z(\vec{r}) = 0 \\ f_2(\vec{r}) = \partial_y B_z(\vec{r}) - \partial_z B_y(\vec{r}) = 0 \\ f_3(\vec{r}) = \partial_z B_x(\vec{r}) - \partial_x B_z(\vec{r}) = 0 \\ f_4(\vec{r}) = \partial_x B_y(\vec{r}) - \partial_y B_x(\vec{r}) = 0 \end{cases} \quad (5)$$

and the same applies to the sum of squares of all four functions:

$$g(\vec{r})^2 \equiv f_1(\vec{r})^2 + f_2(\vec{r})^2 + f_3(\vec{r})^2 + f_4(\vec{r})^2 = 0. \quad (6)$$

If the magnetic field is measured over a volume v , we can define the following magnitude:

$$\xi = \sqrt{\frac{1}{v} \int_v g(\vec{r})^2 dv} \quad (7)$$

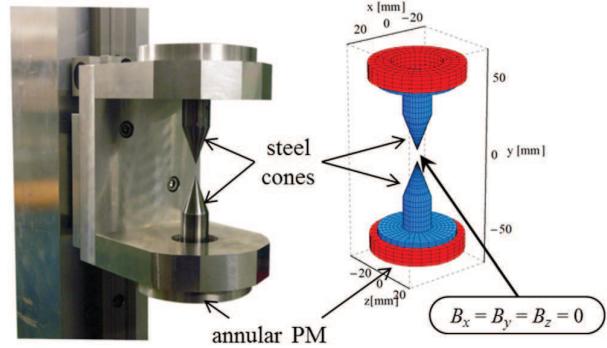


Figure 6. Picture and magnetic model of the system of cones used at ALBA to determine the position of the sensitive area of the Hall probes.

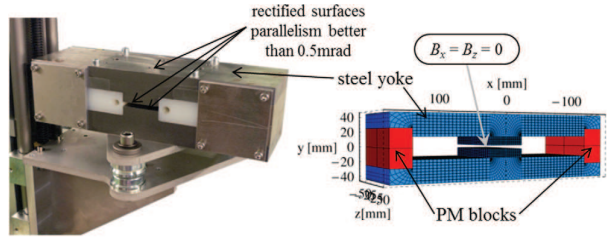


Figure 7. Picture and magnetic model of the alignment dipole used at ALBA to determine the orientation of Hall probes.

and determine the values of the relative displacements between sensors than minimize it. The multidimensional minimization procedure of $\xi(\delta x_b, \delta y_b, \delta z_b, \delta x_c, \delta y_c, \delta z_c)$ is carried out using the conjugated gradient algorithm. By applying the same procedure to volumes corresponding to different magnetic field distributions and comparing the obtained values for the displacements, it is possible to get an estimation of the associated errors. In our case, we have estimated that the accuracy in the determination of the displacements is typically in the order of 50–100 μm .

2.3.5. Absolute positioning of the Hall probe. A method is required to transfer the measured field map from the coordinate system associated with the Hall probe bench to a coordinate system associated with some fiducial marks or mechanical features of the magnet being measured. In order to do so, we have designed a system of magnetic cones defining a point of zero magnetic field at its mechanical centre, as shown in figure 6. The mechanical centre of the cone

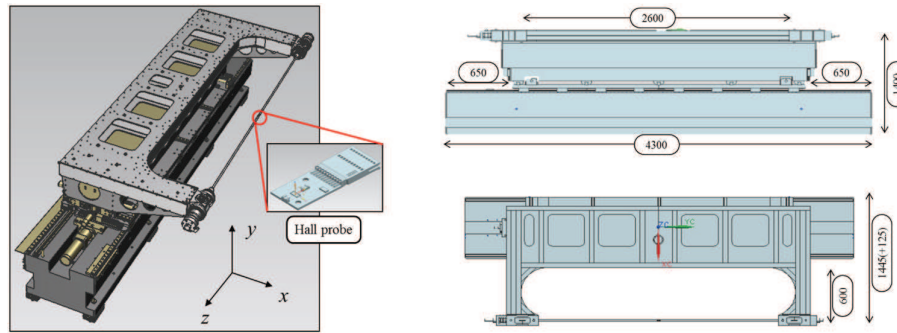


Figure 8. Drawings of the prototype of the Hall probe bench for the measurement of closed structures.

assembly can be determined by means of laser tracker measurements, and its magnetic centre (defined as the point where $B_x = B_y = B_z = 0$) by means of a scan with the Hall probe, allowing us to locate the sensitive area of the Hall probe relative to the coordinate system of the laser tracker.

The system of cones at ALBA generates a field gradient of $14 \mu\text{T } \mu\text{m}^{-1}$ within the horizontal plane and $28 \mu\text{T } \mu\text{m}^{-1}$ along its vertical direction. Therefore, typical magnetic field errors of $10 \mu\text{T}$ give rise to positioning errors smaller than $1 \mu\text{m}$.

2.3.6. Alignment of the Hall probe. In general, it is also necessary to determine the orientation of the Hall probe relative to the vertical direction as defined by gravity. This orientation changes slightly each time the probe is mounted onto the support arm. With this aim, a reference dipole based on permanent magnets has been developed, as shown in figure 7. By construction, the surfaces defining the air gap and the top surface of the magnet are parallel within less than 0.5 mrad . As a consequence, the dipole generates a magnetic field in its air gap perpendicular to its rectified top surface. Therefore, once the top surface of the dipole has been aligned with respect to gravity, a measurement of its magnetic field allows determining the misalignment angle of the Hall probe. It has been determined that this method leads to an alignment accuracy within 0.2 mrad .

3. Latest developments

3.1. New challenges

During recent years, an interest has emerged in developing systems to measure local magnetic field inside closed structures, including superconducting devices, in-vacuum undulators (either cryogenic or room temperature ones), H-type long dipole magnets, etc. All those structures cannot be accessed laterally with a conventional Hall probe bench.

Most of the solutions implemented so far to solve this challenge involve installing the mechanics of the probe driving system inside the aperture of the structure to be measured (see for instance [8–10]). As a consequence, those solutions are very specific for each case.

At ALBA we have been looking for a more general approach to the problem, which would allow using it in a

Table 1. Mechanical specifications and determined performances of the prototype of a Hall probe bench for the measurement of closed structures.

Parameter		Units	Value	
Ranges	x	(mm)	230	
	y	(mm)	90	
	z	(mm)	1280	
Max. on-the-fly speed	v_z	(mm s ⁻¹)	13	
Parameter		Specification	Measured	
Positioning errors (wrt encoder)	x	(μm)	<50	7
	y	(μm)	<50	5
	z	(μm)	<50	10
Angular errors	Roll	(μrad)	<50	35
	Pitch	(μrad)	<50	25
	Yaw	(μrad)	<100	20

wider range of situations. We ended up with a concept based on placing a light Hall probe on top of a stretched flexible tape, passed through the open ends of the measured structure, and driven by an external motion system.

3.2. New Hall bench prototype

In order to validate the concept, it was decided to build a prototype and test its performance [11]. From a mechanical point of view, the prototype would be based on a granite bench providing displacements in all three directions, in a way similar to a conventional Hall probe bench. However, the traditional arm with a Hall probe mounted at its end would be replaced by a C-shape structure stretching a flexible tape between its ends and with a Hall probe placed on it. The flexible tape can be detached from its supporting structure in order to allow passing it through the aperture of the measured system before attaching and stretching it again. The main drawback of such a configuration is that the tape has to be at least two times longer than the structure to be measured, which impacts on the required size of the C-shape structure. Some drawings of the prototype indicating its dimensions are shown in figure 8, and the design specifications are listed in table 1.

The C-shape piece of the prototype is an aluminium profile structure with one tensioning block at each end to hold

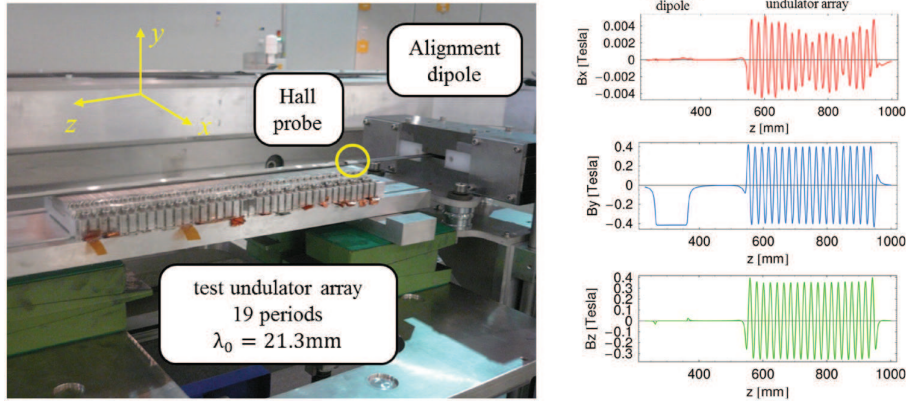


Figure 9. Left: Experimental setup to evaluate the magnetic performance of the prototype bench. Right: Obtained profile for the three components of the magnetic field.

and stretch the flexible tape. One of the tensioning blocks is equipped with a stretch gauge to control the tension applied onto the tape. The total weight of the structure is approximately 400 Kg.

As a material for the flexible tape we have chosen a carbon fibre strip, with a cross section of $16 \times 1.4 \text{ mm}^2$, and a density of 1600 Kg m^{-3} . By design, the nominal tension applied to the tape will be 5 kN, but if necessary it can be increased up to a maximum value of 20 kN.

Regarding the Hall probe, it has a configuration equivalent to other in-house probes produced at ALBA—a circuit board with three orthogonal Hall sensors and a Pt-100 temperature sensor—but with reduced dimensions in order to keep both its thickness and weight as small as possible. The calibration and fiducialization procedures developed for our conventional Hall bench, described in section 2.3, can be also applied to this new bench.

3.2.1. Bench prototype characterization. The bench prototype has been thoroughly characterized from a mechanical point of view using a laser interferometer (Renishaw ML10). The characterization included the determination of performances in terms of positioning (resolution, repeatability, backlash and linearity), guidance (yaw, pitch, roll, flatness and straightness), scanning (following error) and dynamics (resonance frequencies and background noise). The obtained performances, all of them well within specifications, are summarized in the lower part of table 1. It is interesting to note that measured vibrations along the vertical direction had an amplitude well below $1 \mu\text{m}$.

In order to characterize the magnetic performance of the bench, we measured a short undulator array with a period of $\lambda_u = 21.3 \text{ mm}$ and the alignment dipole magnet described in section 2.3.6; in this way the performance of the bench measuring homogeneous and rapidly changing magnetic fields can be compared. The measurement setup and the associated magnetic field profile are shown in figure 9.

Measurements were repeated 10 times and the obtained results compared. Figure 10 shows the measured profile for the vertical component of the magnetic field and the

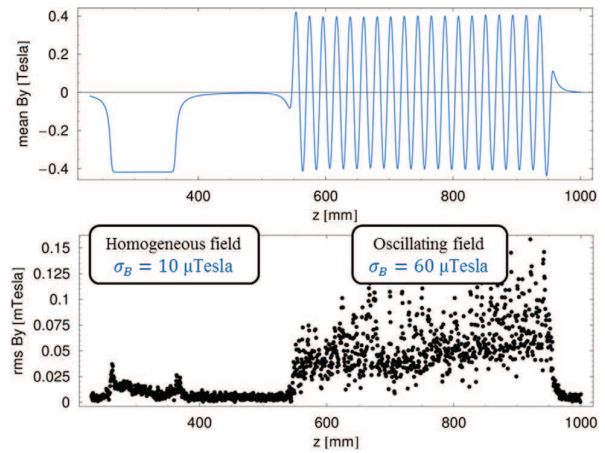


Figure 10. Average value (top) and standard deviation (down) of the vertical component of the magnetic field over 10 repeats.

corresponding rms dispersion of value at each position. It can be seen that, in the homogeneous field region, the system repeatability is $\sim 10 \mu\text{T}$, whereas in the oscillating field region it worsens by up to $\sim 60 \mu\text{T}$.

Regarding the measured field profile of the undulator array, if one identifies the poles as those points where $\partial B_y / \partial z = 0$, the rms error of the pole positions is of the order of $1 \mu\text{m}$, and the rms error of the associated peak field strength is $40 \mu\text{T}$. Finally, it is worth noting that the optical phase error calculated from the field profile is reproducible within 0.01° .

3.3. First results

After having validated its performance at ALBA, on October 2016 the bench prototype was moved to the premises of the CIEMAT Institute in Madrid, with the objective of characterizing the magnet of a compact cyclotron being developed there [12]. The cyclotron magnet will generate a field of 4 T using superconducting NbTi coils at a nominal current of 110 Amp. The aim of the measurements was to check the magnetic field distribution in the good field region of the

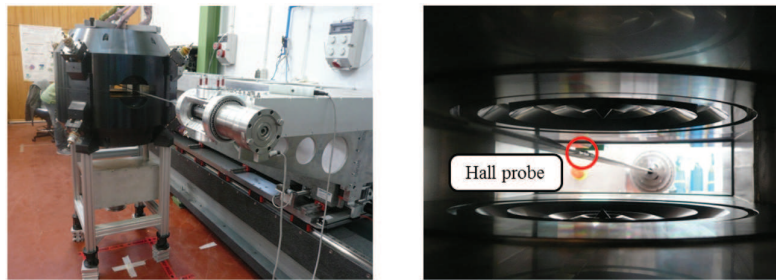


Figure 11. Pictures of the prototype of measurement bench at premises of CIEMAT (Madrid) for the measurement of the magnet of a compact cyclotron.

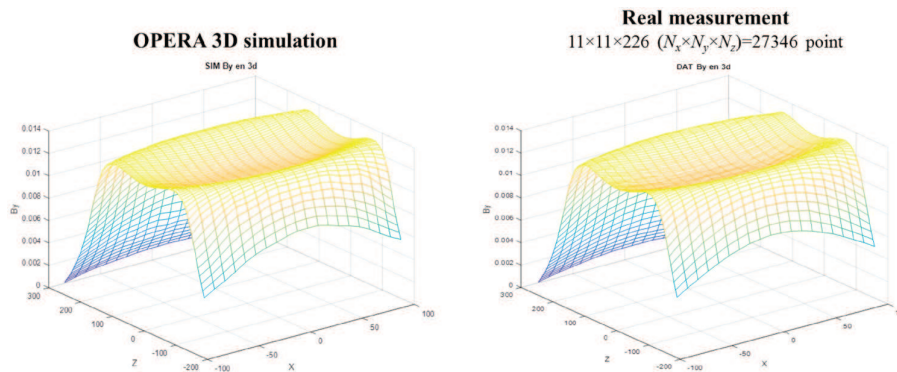


Figure 12. Comparison between the magnetic field profile in the midplane of the cyclotron at 100 mA determined from simulations (left) and experimentally measured using the new Hall probe bench for closed structures (right).

magnet. Figure 11 shows some pictures of the bench prototype after having been installed for the measurement of the cyclotron magnet.

Given that the cryogenic system of the coils is not operational yet, so far only measurements under warm conditions at low currents (up to 100 mA) have been carried out. These preliminary results have been compared with theoretical predictions and, so far, they show a very good agreement. As an example, figure 12 shows the expected field profile within the midplane of the magnet for a current of 100 mA determined from OPERA simulations as compared to a real measurement. Deviations from the model are smaller than 1 mT for the whole volume, with most of the points well below 0.5 mT of deviation.

4. Conclusions

The magnetic measurements laboratory at ALBA is used to test and measure magnetic structures both internally and under request from external institutions and companies. Different experimental techniques are available, for measuring both local and integrated magnetic fields. In particular, one of the principal areas of expertise at ALBA are Hall probe measurements, and over the years several methodological and instrumental developments have been implemented in order to improve the accuracy of our systems. One of the latest developments at ALBA has been a new concept of Hall probe bench devoted to the measurement of closed and small aperture magnetic structures. A proof of concept prototype has

been built and successfully tested, both from a mechanical and magnetic point of view. Obtained results indicate that the performance of the system is analogous to that of a conventional Hall probe bench, thus confirming the feasibility of the proposed solution.

Acknowledgments

The authors wish to thank Fernando Toral and Javier Munilla from CIEMAT for the data of the first test measurements of the cyclotron at CIEMAT.

References

- [1] Einfeld D 2011 ALBA Synchrotron light source commissioning *Proc. IPAC 2011 (San Sebastián, Spain)* pp 1–5 MOAXX01
- [2] Einfeld D, Krüssel A and Pont M 1999 Magnetic measurements of the ANKA storage ring magnets *Proc. 1999 Particle Accelerator Conf. (New York, USA)* pp 3375–7
- [3] Dallin L, Blomqvist I, Lowe D, Swirsky J, Campmany J, Goldie F and Coughlin J 2002 Gradient dipole magnets for the Canadian light source *Proc. EPAC 2002 (Paris, France)* pp 2340–2
- [4] Marcos J, Massana V, Campmany J, Milanese A, Petrone C and Walckiers L 2016 Magnetic measurements of SESAME storage ring dipoles at ALBA *Proc. IPAC 2016 (Busan, Korea)* pp 1148–50 TUPMB018
- [5] Marcos J, Massana V, Campmany J, Castellanos J, Podadera I, Oliver C, Toral F and Nomen O 2016 Detailed characterization of MEBT quadrupoles for the linear IFMIF

- prototype accelerator (LIPAc) *Proc. IPAC 2016 (Busan, Korea)* pp 1151–3 TUPMB019
- [6] Popovic R S 2004 *Hall Effect Devices* (Bristol: IOP Publishing)
- [7] Beltrán D, Bordas J, Campmany J, Molins A, Perlas J A and Traveria M 2001 An instrument for precision magnetic measurements of large magnetic structures *Nucl. Instrum. Methods A* **459** 285–94
- [8] Tanaka T, Tsusu R, Nakajima T, Seike T and Kitamura H 2007 *In situ* undulator field measurement with the SAFALI system *Proc. FEL 2007 (Novosibirsk, Russia)* pp 468–71 WEPPH052
- [9] Chavanne J, Hahn M, Kersevan R, Kitegi C, Penel C and Revol F 2008 Construction of a cryogenic permanent magnet undulator at the ESRF *Proc. EPAC 2008 (Genoa, Italy)* pp 2243–5 WEPC105
- [10] Gerstl S *et al* 2015 First characterization of a superconducting undulator mockup with the CASPER II magnetic measurement system *Proc. IPAC 2015 (Richmond, USA)* pp 2815–7 WEPMA027
- [11] Campmany J, Becheri F, Colldelram C, Marcos J, Massana V and Ribó L 2015 A new bench concept for measuring magnetic fields of big closed structures *Proc. IPAC 2015 (Richmond, USA)* pp 1690–2 TUPJE036
- [12] Oliver C *et al* 2013 Optimizing the radioisotope production with a weak focusing compact cyclotron *Proc. Cyclotrons 2013 (Vancouver, Canada)* pp 429–31 WE4PB03